Journal of Molecular Graphics and Modelling 47 (2014) 18–24

Contents lists available at ScienceDirect

Journal of Molecular Graphics and Modelling

journal homepage: www.elsevier.com/locate/JMGM

P1 and P1′ *para*-fluoro phenyl groups show enhanced binding and favorable predicted pharmacological properties: Structure-based virtual screening of extended lopinavir analogs against multi-drug resistant HIV-1 protease

Ravikiran S. Yedidi[a,1], Zhigang Liu[a,2], Iulia A. Kovari[a], Patrick M. Woster[b], Ladislau C. Kovari[a,*]

[a] Department of Biochemistry and Molecular Biology, School of Medicine, Wayne State University, 540 E. Canfield Avenue, Detroit, MI 48201, USA
[b] Department of Pharmaceutical and Biomedical Sciences, Medical University of South Carolina, 280 Calhoun St., QF305B, Charleston, SC 29425, USA

ARTICLE INFO

Article history:
Accepted 25 October 2013
Available online 1 November 2013

Keywords:
HIV/AIDS
HIV-1 protease
Multidrug-resistance
Protease inhibitors
Lopinavir
Virtual screening

ABSTRACT

Crystal structure of multidrug-resistant (MDR) clinical isolate 769, human immunodeficiency virus type-1 (HIV-1) protease in complex with lopinavir (LPV) (PDB ID: 1RV7) showed altered binding orientation of LPV in the expanded active site cavity, causing loss of contacts and decrease in potency. In the current study, with a goal to restore the lost contacts, three libraries of LPV analogs containing extended P1 and/or P1′ phenyl groups were designed and docked into the expanded active site cavity of the MDR769 HIV-1 protease. The compounds were then ranked based on three criteria: binding affinity, overall binding profile and predicted pharmacological properties. Among the twelve proposed extensions in different combinations, compound **14** (consists of *para*-fluoro phenyl group as both P1 and P1′ moieties) was identified as a lead with improved binding profile, binding affinity against the MDR protease and favorable predicted pharmacological properties comparable to those of LPV. The binding affinity of **14** against wild type (NL4-3) HIV-1 protease was comparable to that of LPV and was better than LPV against an ensemble of MDR HIV-1 protease variants. Thus, **14** shows enhanced binding affinity by restoring lost contacts in the expanded active site cavity of MDR769 HIV-1 protease variants suggesting that it may have higher potency compared to that of LPV and hence should be further synthesized and evaluated against NL4-3 as well as MDR variants of HIV-1.

1. Introduction

Human immunodeficiency virus type-1 (HIV-1) protease [1] is a homo-dimeric aspartyl protease that is critical for the viral replication and maturation [2,3]. Inhibition of the protease would significantly lower the viral infection within the host as well as between the hosts. Among the various generations of protease inhibitors (PI), Kaletra [4,5] has been a very successful combination of the PIs – lopinavir (LVP) and ritonavir (RTV) [6]. As shown in Fig. 1a, both LPV and RTV have similar functional groups at the P1 and P1′ positions with the transition state mimic hydroxyl group [7–9] in between the P1 and P1′.

Previously it has been shown that severe accumulation of mutations causes loss of binding [10] for LPV against the multi-drug resistant (MDR) clinical isolate 769 [11] HIV-1 protease (PDB ID: 1RV7). LPV shows more contacts with wild type (PDB ID: 1MUI) than with MDR769 HIV-1 protease (PDB ID: 1RV7). The MDR769 HIV-1 protease shows a wide-open conformation of the flaps [12] due to conformational rigidity caused by the accumulation of mutations [13]. A similar trend of wide-open flaps consistent in four variants [14] with the MDR769 background was also reported earlier. Mutations from longer side chain residues to shorter side chain residues cause an overall expansion of the active site cavity, which in turn causes weaker binding of the PI due to loss of contacts [10,15]. Recently it has been shown that a scanning Ala/Phe chemical mutagenesis approach can be effectively used to probe the expanded active site cavity of MDR769 HIV-1 protease with peptides [16]. Based on these structural analyses, it was

* Corresponding author at: Department of Biochemistry and Molecular Biology, School of Medicine, Wayne State University, 540 E. Canfield Avenue, Detroit, MI 48201. USA. Tel.: +1 313 993 1335; fax: +1 313 577 2765.
E-mail address: kovari@med.wayne.edu (L.C. Kovari).
[1] Current address: Experimental Retrovirology Section, HIV and AIDS Malignancy Branch, National Cancer Institute, National Institutes of Health, Bethesda, MD 20892, USA.
[2] Current address: Division of Internal Medicine, Harbor Hospital, Baltimore, MD 21225, USA.

1093-3263/$ – see front matter © 2013 Elsevier Inc. All rights reserved.
http://dx.doi.org/10.1016/j.jmgm.2013.10.010

hypothesized that by substituting the P1 and P1′ phenyl groups of LPV with extended analogs of phenyl group one can restore the lost contacts in the expanded active site cavity.

With a goal to restore the lost contacts, 12 extensions were designed as shown in Fig. 1b. The 12 proposed extended analogs were categorized into three libraries. Library #1 (compounds **1**–**12**) consists of asymmetric compounds where the P1′ phenyl group is substituted by the extended analog; library #2 (compounds **13**–**24**) consists of symmetric compounds where both the P1 and P1′ phenyl groups are substituted by the same extended analog and library #3 (compounds **25**–**32**) consists of compounds with combination of extended analogs from libraries 1 and 2 that exhibit improved binding. Virtual screening [17–19] of the compounds was performed using AutoDock-Vina [20] against the MDR769 protease receptor (without ligand) taken from the crystal structures, PDB IDs: 1RV7 and 3OQ7. The compounds were ranked according to their binding affinities (docking score) using the protocol given in Fig. 2 and a lead compound was identified based on a combination of highest binding affinity value, improved overall binding profile and favorable predicted pharmacological properties. The lead compound was further docked into the active site cavity of (i) wild type (NL4-3) HIV-1 protease taken from the crystal structure of NL4-3 HIV-1 protease in complex with LPV [21], (PDB ID: 1MUI), (ii) all the protease–LPV crystal structures available in RCSB PDB (Research Collaboratory for Structural Bioinformatics Protein Data Bank) to date and (iii) an ensemble of MDR variants (PDB IDs: 3OQ7, 3OQA, 3OQD, 3PJ6 and 2RKF). Docking solutions were analyzed in detail. Molecular properties of pharmacological interest, based on Lipinski's rule of five [22], were predicted using molinspiration software (http://www.molinspiration.com) for each of the 32 compounds designed in the current study, in order to verify any violations that may decrease the drug-likeliness of the compound.

2. Materials and methods

2.1. Design and preparation of extended LPV analogs for docking

Extended LPV analogs were designed using ChemDraw and were modeled using the coordinates of LPV taken from the crystal structure, PDB ID: 1MUI, as a template. The compounds were then energy minimized using the Chem3D (http://www.cambridgesoft.com) interface to avoid any bad contacts (steric clashes). Three libraries of compounds were generated. Library#1 consists of asymmetric extensions (compounds **1**–**12**) with an extended phenyl group at P1′ position. Library#2 consists of symmetric extensions (compounds **13**–**24**) with extended phenyl groups at both P1 and P1′ positions. Library#3 consists of combinations of the extensions from libraries 1 and 2 with best binding affinities. The compounds were further prepared for docking using AutoDockTools [23] graphics interface as described previously [15].

2.2. Preparation of the receptor for docking

The crystal structures of MDR769 HIV-1 protease, PDB IDs: 1RV7 and 3OQ7, were chosen as receptors. Coordinates for crystallographic waters and LPV were deleted. Asn25 and Asn125 were modified to Asp25 and Asp125 to represent catalytically active form of the protease followed by the addition of polar hydrogens to the receptor. The three-dimensional docking grid has been generated covering the residues from the active site area, flaps and the 80s loops (Pro79 to Asn83) that are critical in ligand binding. This receptor grid was generated using the AutoDockTools graphics interface and the same grid was used for docking all the compounds one at a time. Vina [20] program was used to perform the fast pace exhaustive conformational searching for each of the designed compounds.

2.3. Virtual screening, ranking and prediction of pharmacological properties for the extended LPV analogs

The binding pose with the highest binding affinity (out of the top five poses) for each compound was chosen and binding orientation was analyzed. Final ranking of the compounds was performed as described in Fig. 2. Molecular properties of pharmacological interest (based on Lipinski's rule of five) for each compound were calculated using molinspiration software (http://www.molinspiration.com).

2.4. Structural analysis

All the protease-drug interactions were calculated as described previously [15]. A cut-off of 3 Å distance between the donor and acceptor, 90° angle for the donor and 60° for the acceptor were used for the calculation of hydrogen bonds. The hydrophobic contacts were computed between the two carbon atoms (one from the protease residue and the other from LPV/LPV analog) within a distance of 4 Å. Figs. 1, 4a and S3 were prepared using ChemDraw Ultra (http://www.cambridgesoft.com); Fig. 5 was generated using the open source molecular graphics program, PyMol (v0.99) (http://www.pymol.org).

3. Results

3.1. Virtual screening of extended LPV analogs

Among the 24 compounds from libraries 1 and 2 used for the virtual screening of the expanded active site cavity of the MDR protease, compound **14** was identified as the lead compound with highest binding affinity and improved overall binding profile. As shown in Fig. 3, a total of 22 extended LPV analogs (**1**–**20**, **22** and **23**) show better binding affinity values compared to that of LPV (−6.7 kcal/mol) screened against the MDR protease. Compounds **24** and **21** showed lowest binding affinity values −6.6 kcal/mol and −5.9 kcal/mol, respectively among the 24 compounds.

3.2. Binding affinities of asymmetric compounds (library–1)

Virtual screening of the asymmetric series of compounds (**1**–**12**) with an extended phenyl analog at the P1′ position yielded three compounds (**1**, **6** and **11**) with highest binding affinity within library #1. Among the asymmetric series, the *para*-methyl extension at P1′ position of LPV (compound **1**) was chosen as the lead compound with best binding affinity and overall improved binding profile. Compounds **6** and **11**, in spite of improved binding, were not chosen due to their relatively higher molecular weight. The highest binding affinity value among this series was −7.7 kcal/mol (compound **1**) and the lowest was −6.9 kcal/mol for the compounds **7**, **9** and **12** (Fig. 3).

3.3. Binding affinities of symmetric compounds (library–2)

The symmetric series of compounds (**13**–**24**) have the same extended phenyl analog at both P1 and P1′ positions on LPV template. Virtual screening of the symmetric series of compounds yielded one compound, **14**, with highest binding affinity. Among the symmetric series, compound **14**, with *para*-fluoro extensions at both P1 and P1′ positions of LPV shows best binding affinity (−7.8 kcal/mol) and was chosen as the lead compound within the library #2. As shown in Fig. 3, the highest and lowest binding affinity values among this series are −7.8 kcal/mol and −5.9 kcal/mol for **14** and **21**, respectively.

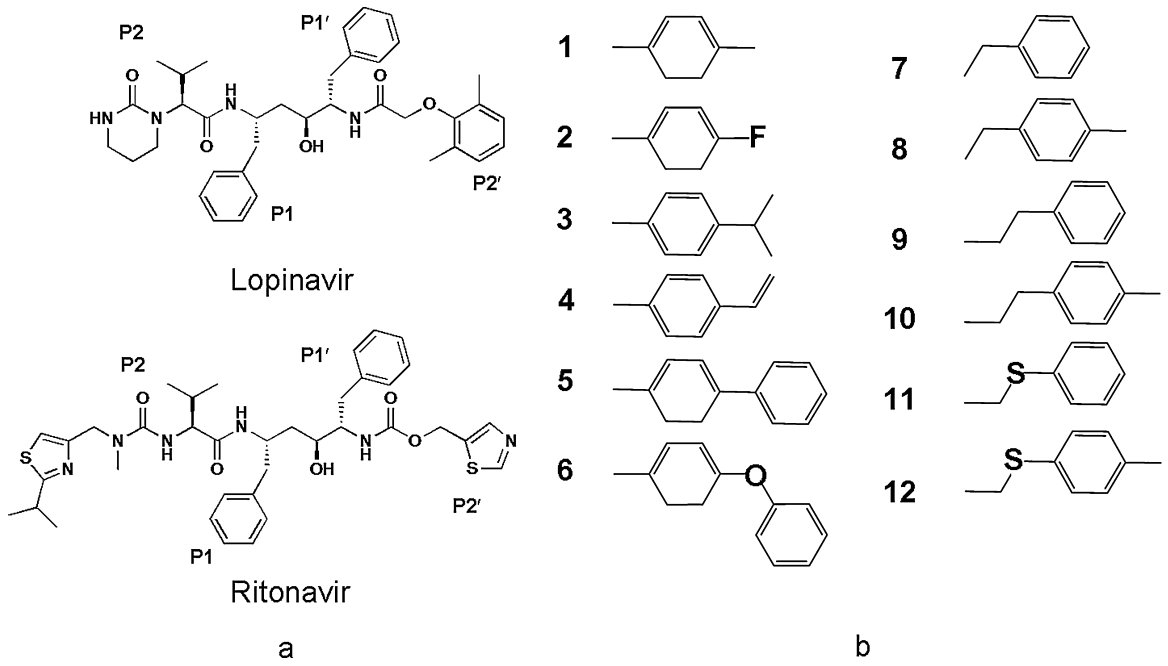

Fig. 1. Structures of lopinavir, ritonavir and extended phenyl analogs. Structures of lopinavir and ritonavir (components of Kaletra) labeled with the P2, P1, P1′ and P2′ functional groups are shown in panel a. The 12 extended phenyl analogs proposed in the current study are shown in panel b. The phenyl groups at P1 and P1′ of lopinavir are substituted with the extended phenyl analogs in a combinatorial fashion to analyze the binding affinities as well as the overall binding profiles of the extended-lopinavir analogs by docking and scoring.

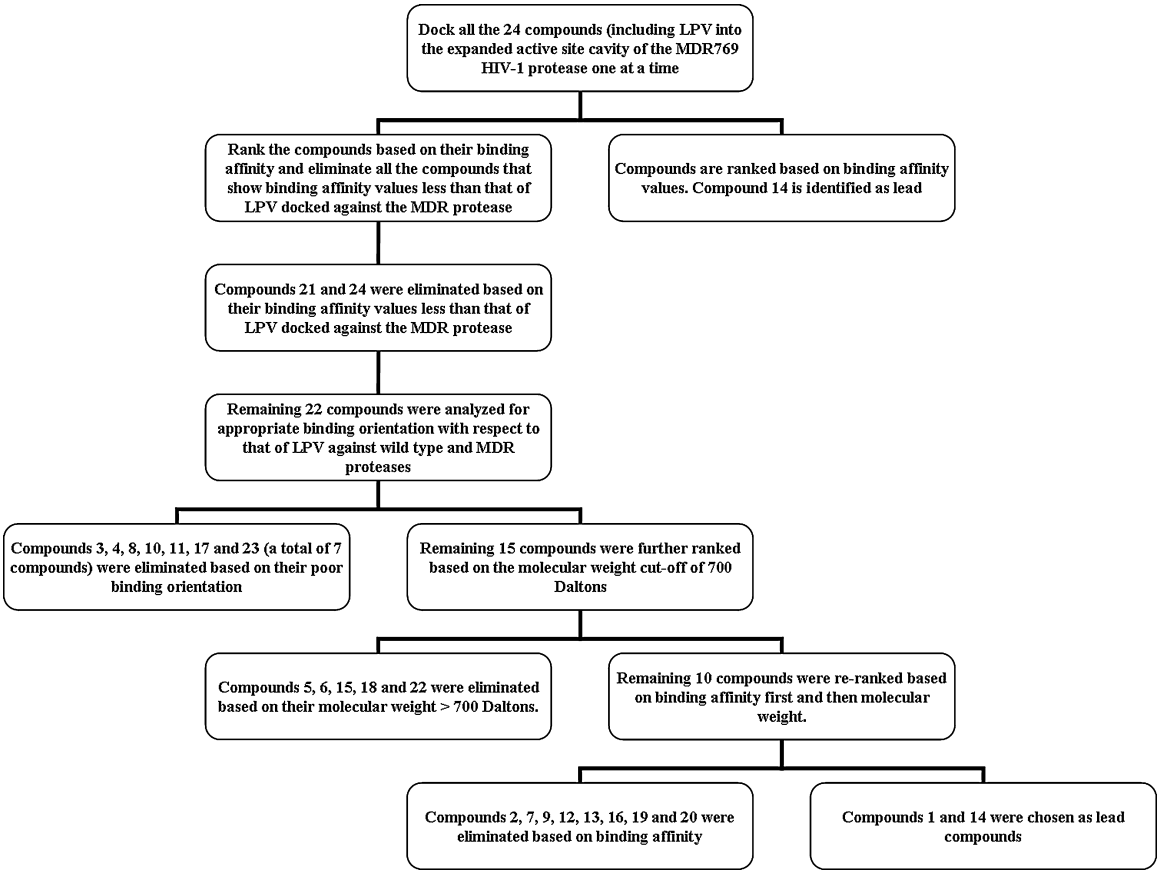

Fig. 2. Flow chart showing sorting and ranking of extended LPV analogs, compounds **1**–**24** from libraries 1 and 2 docked against the expanded active site cavity of the MDR769 HIV-1 protease.

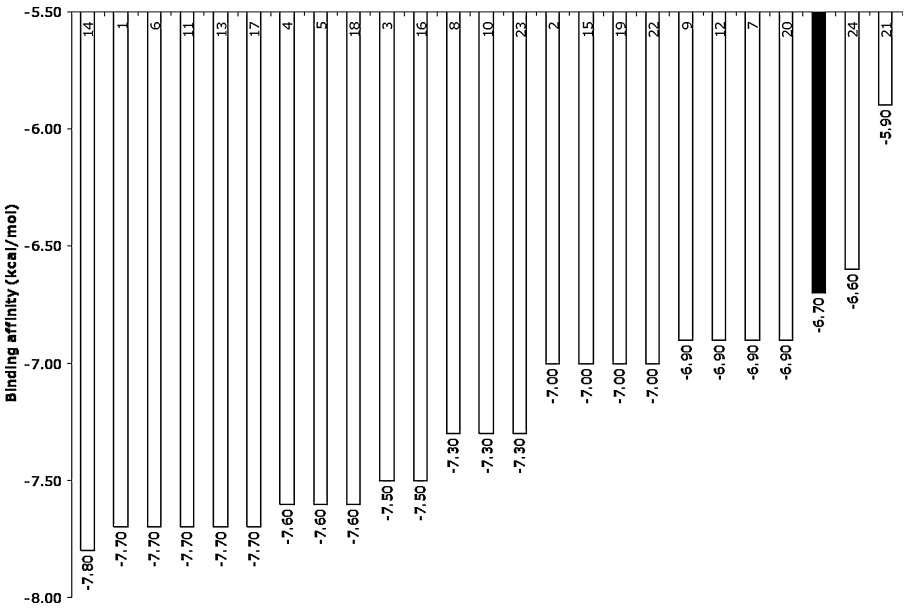

Fig. 3. Binding affinities of extended lopinavir analogs. The binding affinity (kcal/mol) values of extended lopinavir analogs (compounds **1**–**24**), docked against the MDR769 HIV-1 protease receptor, are plotted on the *y*-axis from highest on the left to the lowest on the right as white bars. Lopinavir is highlighted as a black bar. Individual binding affinity values are listed at the bottom of each bar. Compound **14** shows highest binding affinity and was identified as lead compound in the current study.

3.4. Binding affinities of combinations (library–3)

The modifications 1, 2, 5, 6 and 11 (Fig. 1b) were chosen based on their higher binding affinity values and improved binding profiles from libraries 1 and 2 to mix and match as combinations in library–3. Combinations of the extensions 1, 2, 5, 6 and 11 at P1 and P1′ positions did not improve the binding affinity any better than that of **14**. As shown in Table S1, the combinations among the best five extended analogs yielded binding affinity values between −7.7 kcal/mol and −7.1 kcal/mol. Thus further exploration of the combinations was stopped because of the higher molecular weight. The combination of extensions 2 and 11 (compound **27**) was chosen as the lead from this library because of its relatively lower molecular weight, improved overall binding profile and higher binding affinity.

3.5. Binding affinity of lead compound against wild type and MDR protease variants

The chemical structure of the lead compound (**14**) is shown in Fig. 4a. As shown in Fig. 4b, LPV re-docked into the active site cavity of the wild type HIV-1 protease (PDB: 1MUI) yielded a binding affinity of −10.3 kcal/mol but when docked into the expanded active site cavity of the MDR protease, yielded a binding affinity of −6.7 kcal/mol. Thus, LPV showed a loss of 3.6 kcal/mol in its binding affinity against MDR protease. On the other hand, **14** showed a loss of 2.6 kcal/mol in its binding affinity against MDR protease but improved binding profile. **14** shows better binding affinity against both the wild type (−10.4 kcal/mol) and the MDR (−7.8 kcal/mol) proteases compared to LPV. The models created by docking **14** against wild type and MDR protease were also

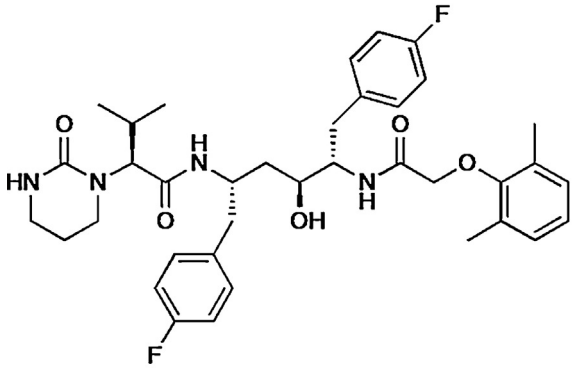

Compound **14**

a

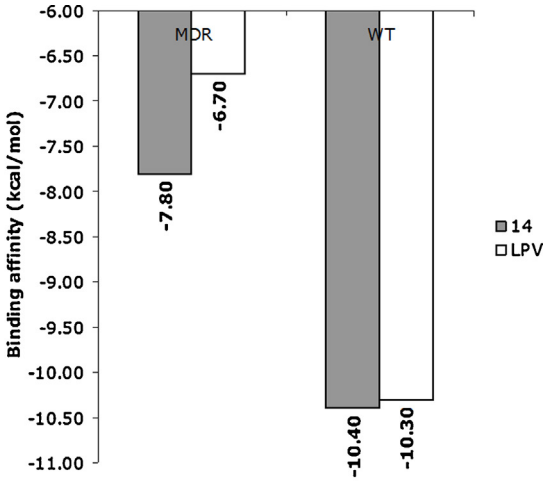

b

Fig. 4. Structure and binding affinity of lead compound. Structure of the lead compound, **14**, is displayed in panel a. Compound **14** has symmetric *para*-fluoro extensions at P1 and P1′ with lopinavir backbone. In panel b, binding affinity of the lead compound (gray bars) is compared to that of lopinavir (white bars) docked against the wild type and the MDR strains of HIV-1 protease, respectively. As shown in panel b, the lead compound shows better binding affinity than LPV against MDR receptor (with wide-open flaps) and comparable binding affinity against wild type receptor (with closed flaps).

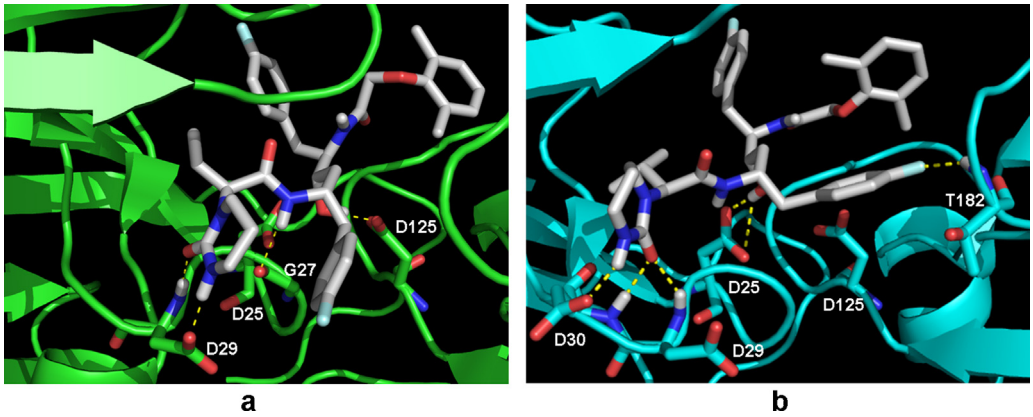

Fig. 5. Hydrogen bonding network for compound **14**. Models of wild type (green color) and MDR769 (cyan color) HIV-1 protease docked with **14** (shown as white stick model) are shown in panels a and b, respectively. Polar contacts are shown as yellow dashed lines. Protease residues that are involved in polar contacts are highlighted as stick models in both panels. Compound **14** shows 4 and 6 polar contacts in wild type and MDR protease models, respectively. Restoration of lost contacts in the S2 binding pocket (D29 and D30) is shown in panel b. The P2 cyclic urea moiety of **14** shows two polar contacts with D29 in wild type model and three polar contacts (two with protease backbone and one with the side chain of D30) in the MDR model. An additional contact between the *para*-fluoro from P1 group of **14** and the backbone amide nitrogen atom of T82 is seen in the MDR model.

Table 1
Binding profiles of LPV and **14** docked against NL4-3 and MDR769 HIV-1 protease variants. Compound **14** shows higher binding affinity values as well as higher number of contacts with both NL4-3 and MDR.

Protease	Compound	Binding affinity (kcal/mol)	Number of polar contacts	Number of hydrophobic contacts	Number of total contacts
NL4-3	**14**	−10.4	4	30	34
	LPV	−10.3	8	21	29
MDR769	**14**	−7.8	6	27	33
	LPV	−6.7	2	18	20

analyzed for contacts. Details of polar and hydrophobic contacts for **14** and LPV are shown in Table 1. As shown in Fig. 5, **14** restored almost all the lost contacts against the MDR protease. Compound **14** was further docked into the active site cavity of MDR HIV-1 protease variants using crystal structures – PDB IDs: 3OQ7, 3OQA, 3OQD, 1TW7, 3PJ6 and 2RKF as receptors and the binding affinities were compared. As shown in Fig. 6, the binding affinity values of **14** are better when compared to those of LPV against all six variants of MDR769 HIV-1 protease. As shown in Fig. 7, the binding affinity of compound **14** is comparable to that of LPV docked against all the protease receptors, in complex with LPV, published

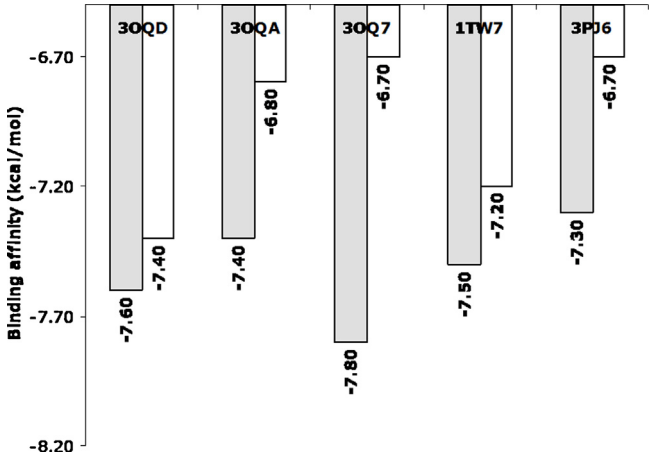

Fig. 6. Binding affinity of lead compound against MDR variants. Binding affinity values of lead compound (**14**) (gray bars) and LPV (white bars) docked against MDR 769 HIV-1 protease crystal structures, PDB IDs: 3OQD, 3OQA, 3OQ7, 1TW7, and 3PJ6 are shown here. The lead compound shows enhanced binding affinity against all MDR variants when compared to LPV.

to date. Protease sequence alignment for all the crystal structures in complex with LPV published to date is shown in Fig. S2.

3.6. Analysis of predicted pharmacological properties for the extended LPV analogs

As shown in Table 2, analysis of predicted molecular properties that are of pharmacological interest (based on Lipinski's rule of five) for each compound revealed that out of 32 compounds from the three libraries, 8 compounds (**17**, **18**, **23**, **24**, **29**, **30**, **31** and **32**) have molecular weights greater than 721 Da (equivalent to molecular weight of ritonavir, which has highest molecular weight among the FDA approved HIV-1 protease inhibitors) and 19 compounds (**3**, **5**, **6**, **10**, **15**, **16**, **17**, **18**, **19**, **20**, **21**, **22**, **23**, **24**, **28**, **29**, **30**, **31** and **32**) show log *P* values greater than 6.7 (equivalent to log *P* value of tipranavir, which has highest log *P* value among the FDA approved HIV-1 protease inhibitors). Among the remaining compounds, **14** was ranked as the compound with highest binding affinity, improved overall binding profile with reasonable pharmacological properties. As shown in Table 2, the predicted pharmacological properties of **14** were comparable to those of the FDA approved HIV-1 protease inhibitors. **14** has molecular weight value less than those of saquinavir, atazanavir and ritonavir. **14** shows similar log *P* values as that of ritonavir and better log P values compared to that of tipranavir.

4. Discussion

The current structure-based virtual screening of extended LPV analogs confirmed the hypothesis that by using extensions at P1 and/or P1′, one can restore the lost contacts in the expanded active site cavity of MDR769 HIV-1 protease. Virtual screening [17] of compounds using crystal structures [18,19] as receptors by docking and scoring is one of the most commonly used methods to identify hits and subsequently, lead compounds especially for drug

Table 2
Predicted molecular properties of lead compound, **14**, are listed along with the FDA approved HIV-1 protease inhibitors (PIs) in the table. The values for each property for the approved PIs were taken from the PubChem database while the predicted values for **14** were calculated using molinspiration software. The compounds are listed in the ascending order of their molecular weight. Compound **14** shows a similar profile to those of the FDA approved PIs.

Compound	Molecular property				
	Mol. Wt.	Log *P*	Number of H-bond donors	Number of H-bond acceptors	Total polar surface area
APV	505.63	2.90	3	8	140
DRV	547.66	2.90	3	9	149
NFV	567.78	5.70	4	5	127
TPV	602.66	6.70	2	10	114
IDV	613.79	2.80	4	7	118
LPV	628.81	5.69	4	9	120
14	664.79	6.02	4	9	120
SQV	670.84	4.20	5	7	167
AZV	704.86	5.60	5	9	171
RTV	720.94	6.00	4	5	202

targets such as HIV-1 protease. In the current study, crystal structure of MDR769 HIV-1 protease, with expanded active site cavity and wide-open flaps, was used as a receptor to perform virtual screening of extended LPV analogs. The scoring method shown in Fig. 2 was used to evaluate the docking poses in order to rank the compounds based on their binding affinity as well as the overall binding profile. In order to emphasize the importance of safety along with the potency of the lead compounds in the pre-clinical drug discovery, predicted pharmacological properties based on Lipinski's rule of five were also used in scoring and ranking.

Exhaustive conformational search of ligand docked in the chemical space (binding site/active site of the receptor) may help in understanding the entropic flexibility of ligand binding. NL4-3 HIV-1 protease shows a closed conformation of flaps upon ligand binding thus decreasing the total volume of chemical space in the active site cavity but, in the case of MDR769 HIV-1 protease variants, due to the conformational rigidity of the wide-open flaps, the overall volume of the active site cavity is higher. Due to the increase in volume of the active site cavity, the LPV molecule has relatively larger chemical space to explore until it finds the best combination of the contacts within the active site cavity for stable binding as seen in the case of PDB ID: 1RV7. Due to this reason, the overall binding orientation (respective positions of the P2, P1, P1′ and P2′ functional groups) of LPV is altered in the MDR protease active site when compared to that of the wild type protease (PDB ID: 1MUI). In order to achieve a stable binding orientation with enhanced binding affinity, the exhaustive conformational search protocol was used from the program Vina for each of the 32 proposed LPV analogs. In the case of **14**, stable conformations with multiple contacts were obtained for both the NL4-3 and MDR receptors. The binding affinity of **14** is not only good against the MDR protease but also higher than that of the LPV against the wild type protease as well as other MDR variants. This re-confirms the hypothesis that by extending the P1 and/or P1′ phenyl groups of LPV, the binding affinity as well as the overall binding profile can be enhanced against the MDR protease, there by restoring the lost contacts.

Distortions in the binding pockets of the MDR769 HIV-1 protease variants cause loss of contacts with the protease inhibitors

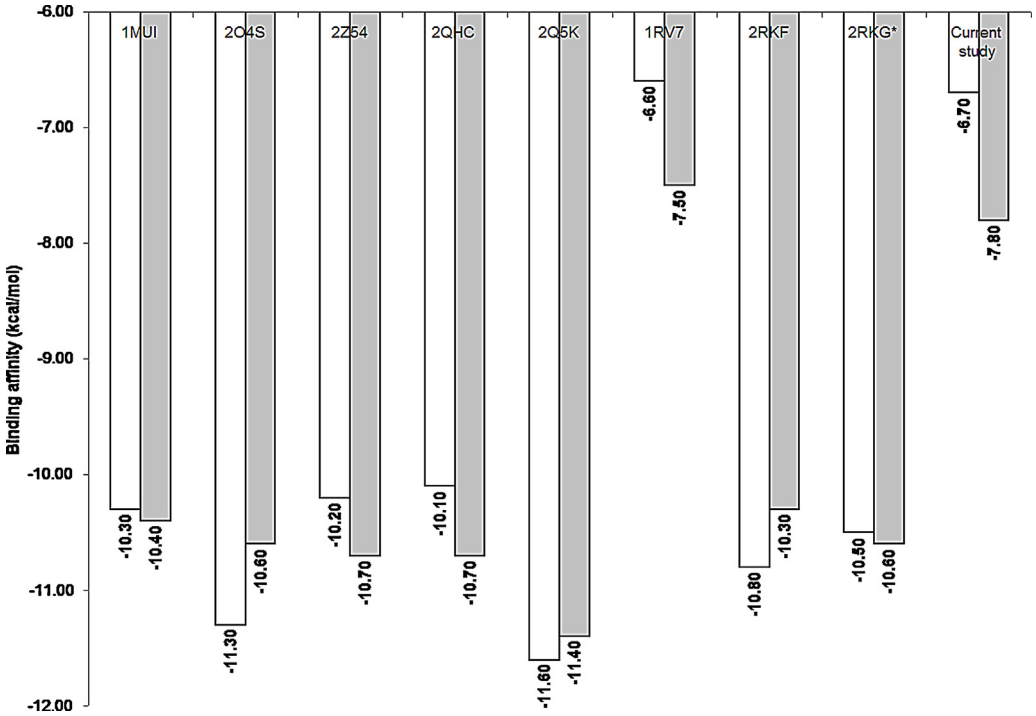

Fig. 7. Binding affinity of lead compound against protease–LPV structures published in the protein data bank. The binding affinity values of **14** (gray bars) and LPV (white bars) docked against all the available protease crystal structures in complex with LPV (taken from the protein data bank) are shown here. Compound **14** shows comparable binding affinity values as those of LPV.

resulting in drug resistance. In such cases, the enzyme-substrate, induced-fit is lost due to altered substrate binding resulting in decreased substrate hydrolysis. On the other hand, if the substrate cleavage site consists of compensatory mutations, the induced-fit can be restored and such MDR strains are propagated further. With a goal to restore the lost contacts and enhance the potency, various extended phenyl analogs were proposed at P1 and P1′ positions of LPV (Fig. 1b) to mimic the compensatory mutations of substrate that may enhance the binding affinity. It was hypothesized that if the P1 and P1′ of LPV are substituted with extended phenyl analogs, one can restore the lost contacts in the S1 and S1′ binding pockets and that the restoration of lost contacts in S1 and S1′ pockets should automatically force the new LPV analog to position the P2 and P2′ functional groups in their corresponding S2 and S2′ pockets of the MDR protease. Docked model of MDR protease with the lead compound, **14** confirmed this hypothesis. As shown in Fig. 5b and Table 1, compound **14**, with *para*-fluoro extensions at P1 and P1′, shows restoration of contacts in the S1 and S1′ pockets, thus forcing the P2 and P2′ functional groups to position in their corresponding S2 and S2′ binding pockets. The P2 (cyclic urea) group of compound **14** shows three direct polar contacts (one with backbone amide nitrogen atom of Asp29, one with backbone nitrogen atom of Asp30 and one with side chain hydroxyl group of Asp 30). These three direct polar contacts replace the bridging water molecules seen in the crystal structure of MDR769 HIV-1 protease variant, PDB ID: 3R0W.

Fluorinated compounds (Fig. S3) are often used as drugs [24,25]. Strategically designed fluorinated compounds not only enhance the bioavailability but also can reduce side effects. Previously it has been shown that the secondary metabolism of LPV includes hydroxylation of the aromatic rings in the diphenyl core of LPV [26]. Addition of *para*-fluoro group to the aromatic rings of the diphenyl core as in the case of **14**, may or may not alter the metabolism severely because often times, compounds are de-fluorinated during metabolism [27]. Thus, **14**, in combination with RTV (as cytochrome P_{450} – 3A4 inhibitor) is predicted to have better efficacy to a wide range of HIV-1 protease strains as well as good pharmacological properties with relatively similar mechanism of metabolism as LPV.

In summary, virtual screening of the MDR protease using a library of 32 compounds built on LPV template with extended phenyl analogs yielded a lead compound (compound **14**) which showed enhanced binding affinity and improved overall binding profile against not only the wild type protease but also the MDR protease variants. Compound **14** with extended P1 and P1′ *para*-fluoro functional groups, is a potential lead compound to target the multidrug-resistant strains of HIV-1 protease such as the MDR769 clinical isolate with distorted binding pockets. Thus, **14** has been selected for further synthesis and evaluation of its antiviral potency.

Acknowledgments

We thank the National Institutes of Health for funding to LCK (Grant # AI065294). We thank Keyur Parikh and Walter Chou (summer interns) for their contributions in synthesis of compound **14** for further evaluation.

Appendix A. Supplementary data

Supplementary material related to this article can be found, in the online version, at http://dx.doi.org/10.1016/j.jmgm.2013.10.010.

References

[1] M.A. Navia, P.M.D. Fitzgerald, B.M. McKeever, et al., Three-dimensional structure of aspartyl protease from human immunodeficiency virus HIV-1, Nature 337 (1989) 615–620.
[2] N.E. Kohl, E.A. Emini, W.A. Schleif, et al., Active human immunodeficiency virus protease is required for viral infectivity, Proc. Natl. Acad. Sci. USA 85 (1988) 4686–4690.
[3] C. Peng, B.K. Ho, T.W. Chang, N.T. Chang, Role of human immunodeficiency virus type 1-specific protease in core protein maturation and viral infectivity, J. Virol. 63 (1989) 2550–2556.
[4] H.L. Sham, D.J. Kempf, A. Molla, ABT-378, a highly potent inhibitor of the human immunodeficiency virus protease, Antimicrob. Agents Chemother. 42 (1998) 3218–3224.
[5] R.S. Cvetkovic, K.L. Goa, Lopinavir/ritonavir: a review of its use in the management of HIV infection, Drugs 63 (2003) 769–802.
[6] D.J. Kempf, K.C. Marsh, G. Kumar, et al., Pharmacokinetic enhancement of inhibitors of the human immunodeficiency virus protease by coadministration with ritonavir, Antimicrob. Agents Chemother. 41 (1997) 654–660.
[7] F. Lebon, M. Ledecq, Approaches to the design of effective HIV-1 protease inhibitors, Curr. Med. Chem. 7 (2000) 455–477.
[8] J.T. Nguyen, Y. Hamada, T. Kimura, Y. Kiso, Design of potent aspartic protease inhibitors to treat various diseases, Arch. Pharm. (Weinheim) 341 (2008) 523–535.
[9] D.H. Rich, Pepstatin-derived inhibitors of aspartic proteinases. A close look at an apparent transition-state analogue inhibitor, J. Med. Chem. 28 (1985) 263–273.
[10] B.C. Logsdon, J.F. Vickrey, P. Martin, et al., Crystal structures of a multidrug-resistant human immunodeficiency virus type 1 protease reveal an expanded active-site cavity, J. Virol. 78 (2004) 3123–3132.
[11] S. Palmer, R.W. Shafer, T.C. Merigan, Highly drug-resistant HIV-1 clinical isolates are cross-resistant to many antiretroviral compounds in current clinical development, AIDS 13 (1999) 611–667.
[12] P. Martin, J.F. Vickrey, G. Proteasa, et al., Wide-open 1.3 Å structure of a multidrug-resistant HIV-1 protease as a drug target, Structure 13 (2005) 1887–1895.
[13] L. Galiano, F. Ding, A.M. Veloro, et al., Drug pressure selected mutations in HIV-1 protease alter flap conformations, J. Am. Chem. Soc. 131 (2009) 430–431.
[14] R.S. Yedidi, G. Proteasa, J.L. Martinez, et al., Contribution of the 80s loop of HIV-1 protease to the multidrug-resistance mechanism: crystallographic study of MDR769 HIV-1 protease variants, Acta Crystallogr. D Biol. Crystallogr. 67 (2011) 524–532.
[15] R.S. Yedidi, Z. Liu, Y. Wang, et al., Crystal structures of multidrug-resistant HIV-1 protease in complex with two potent anti-malarial compounds, Biochem. Biophys. Res. Commun. 421 (2012) 413–417.
[16] R.S. Yedidi, J.M. Muhuhi, Z. Liu, et al., Design, synthesis and evaluation of a potent substrate-analog peptide-inhibitor identified by scanning Ala/Phe chemical mutagenesis, mimicking substrate co-evolution, against multidrug-resistant HIV-1 protease, Biochem. Biophys. Res. Commun. 438 (2013) 703–708.
[17] W.P. Walters, M.T. Stahl, M.A. Murcko, Virtual screening – an overview, Drug Discov. Today 3 (1998) 160–178.
[18] R.T. Kroemer, Structure-based drug design: docking and scoring, Curr. Protein Pept. Sci. 8 (2007) 312–328.
[19] C.N. Cavasotto, A.J.W. Orry, Ligand docking and structure-based virtual screening in drug discovery, Curr. Top. Med. Chem. 7 (2007) 1006–1014.
[20] O. Trott, A.J. Olson, AutoDock Vina: improving the speed and accuracy of docking with a new scoring function, efficient optimization and multithreading, J. Comput. Chem. 31 (2010) 455–461.
[21] V. Stoll, W. Qin, K.D. Stewart, et al., X-ray crystallographic structure of ABT-378 (Lopinavir) bound to HIV-1 protease, Bioorg. Med. Chem. 10 (2002) 2803–2806.
[22] C.A. Lipinski, F. Lombardo, B.W. Dominy, P.J. Feeney, Experimental computational approaches to estimate solubility and permeability in drug discovery and development settings, Adv. Drug Deliv. Rev. 46 (2001) 3–26.
[23] M.F. Sanner, Python: a programming language for software integration development, J. Mol. Graph. Model. 17 (1999) 55–84.
[24] S.G. DiMagno, H. Sun, The strength of weak interactions: aromatic fluorine in drug design, Curr. Top. Med. Chem. 6 (2006) 1473–1482.
[25] F.M.D. Ismail, Important fluorinated drugs in experimental and clinical use, J. Fluorine Chem. 118 (2002) 27–33.
[26] G.N. Kumar, V.K. Jayanti, M.K. Johnson, et al., Metabolism and disposition of the HIV-1 protease inhibitor lopinavir (ABT-378) given in combination with ritonavir in rats, dogs, and humans, Pharm. Res. 21 (2004) 1622–1630.
[27] B.K. Park, N.R. Kitteringham, P.M. O'Neil, Metabolism of fluorine-containing drugs, Annu. Rev. Pharmacol. Toxicol. 41 (2001) 443–470.